# Influence of Morphology on Rheological and Mechanical Properties of SEBS-Toughened, Glass-Bead-Filled Isotactic Polypropene

**F. STRICKER, C. FRIEDRICH, R. MÜLHAUPT**

Freiburger Materialforschungszentrum und Institut für Makromolekulare Chemie der Albert-Ludwigs-Universität, Stefan-Meier-Straße 21, D-79104 Freiburg i. Br., Germany

*Received 30 July 1997; accepted 21 February 1998*

**ABSTRACT:** The influence of morphology of glass-bead-filled isotactic polypropene containing 0–20 vol% thermoplastic elastomers (TPE) on mechanical and rheological properties was investigated. Polystyrene-*block*-poly(ethene-*co*-but-1-ene)-*block*-polystyrene (SEBS) and the corresponding block copolymer grafted with maleic anhydrid (SEBS-*g*-MA) were used as thermoplastic elastomers, realizing, in the first case, a three-phase morphology with separately dispersed glass beads and SEBS particles. In the second case, SEBS-*g*-MA forms an elastomeric interlayer between glass beads and polypropene matrix, comprising core–shell particles. Young's modulus and tensile yield stress of the hybrid composites decrease with an increase in TPE volume fraction due to low stiffness and strength of TPE. In comparison with the three-phase morphology of hybrid composites with SEBS, SEBS-*g*-MA interlayers effect a reduced stiffness of the hybrid composites but improve interfacial adhesion and, thus, tensile yield stress. Rheological storage and loss moduli increase with an increase in glass bead and TPE volume fraction. Due to improved interfacial adhesion, melt elasticity and viscosity are enhanced by the SEBS-*g*-MA interlayer when compared with separately dispersed SEBS. Consequently, the reduced stiffening effect of the glass beads due to SEBS-*g*-MA interlayer decreases mechanical elasticity, whereas improved interfacial adhesion, also promoted by the SEBS-*g*-MA interlayer, enhances tensile yield stress and melt elasticity.
 J Appl Polym Sci 69: 2499–2506, 1998

**Key words:** isotactic propypropene; hybrid composites; morphology; rheology; mechanical properties

## INTRODUCTION

In order to improve mechanical properties of isotactic polypropene (i-PP) and other polymers, it is common practice to incorporate fillers.[1,2] Fillers usually improve stiffness, strength, hardness, and abrasion resistence of i-PP but simultaneously reduce its impact strength. In contrast, elastomers, for example, ethene/propene (EPR), ethene/propene/diene (EPDM), and polystyrene-*block*-poly(ethene-*co*-but-1-ene)-*block*-polystyrene (SEBS) rubber act as impact modifiers for i-PP but reduce its stiffness.[2] It has been the subject of many investigations to combine fillers and elastomers in order to produce i-PP hybrid composites with an improved stiffness–toughness balance.[3–6] Moreover, addition of fillers and elastomers also alters melt flow behavior and, thus, processability of i-PP. The influence of rheological and mechanical properties of polymer, elastomer, and filler on the rheological properties of the composites is investigated well, including the role of elastomers.[2,7,8] However, only little attention has been paid to

*Correspondence to:* F. Stricker.

Journal of Applied Polymer Science, Vol. 69, 2499–2506 (1998)
 CCC 0021-8995/98/122499-08

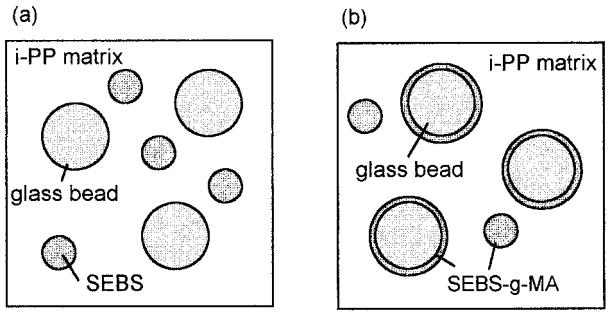


**Figure 1** Morphologies of i-PP hybrid composites: (a) three-phase morphology with separately dispersed elastomer and filler particles, and (b) two-phase morphology with core–shell particles (filler particle core and an elastomeric shell) and separately dispersed elastomer and filler particles.

the contributions of an interfacial shell around the filler particles, although flow properties strongly depend on the interfacial conditions.[9,10] Interfacial shells could result from immobilization of the adjacent polymer matrix due to strong interfacial interactions or from a separate elastomer phase surrounding the filler particles, forming core–shell particles. Previous work[5] has demonstrated that i-PP hybrid composites with glass beads and SEBS have a three-phase morphology with separate dispered glass beads and SEBS particles, whereas a corresponding block copolymer grafted with maleic anhydrid (SEBS-*g*-MA) and glass beads form core–shell particles, where the glass beads are encapsulated *in situ* in a SEBS shell. Figure 1 schematically shows the 2 different morphologies.

The elastomeric SEBS-*g*-MA interlayer strongly influences mechanical properties, as well as crystallization behavior. In comparison to the three-phase morphology, core–shell morphologies exhibit higher yield stress, which reflects improved interfacial adhesion. Moreover stiffness and nucleation ability of the encapsulated glass beads are reduced.

It was the aim of this research to investigate the influence of elastomeric interlayers on mechanical, dynamic mechanical, and rheological properties of SEBS-toughened, glass-bead-filled i-PP. Aminopropyl-functionalized glass beads of 5 $\mu$m average diameter were blended together with i-PP and SEBS in a twin-screw kneader with counterrotating screws at 60 rpm and 240°C. Morphology, rheological, dynamic mechanical, and mechanical properties, for example, stiffness and tensile yield stress, were studied as a function of type and volume fraction of SEBS.

## EXPERIMENTAL

### Materials

All polymers were commercial grades, supplied by Shell, and used without further purification, as follows: isotactic polypropene (i-PP; KM 6100, $M_w$ = 285,900 g/mol; $M_w/M_n$ = 4.9, MFI = 3.5 g/10 min at 230°C; $\eta_0$(200°C) = 40,600 Pa·s), polystyrene-*block*-poly(ethene-*co*-but-1-ene)-*block*-polystyrene (Kraton G1652, abbreviated as SEBS, $M_n$ = 90.000 g/mol, polystyrene content of 29 wt %; $\eta_0$(200°C) = 130,400 Pa·s) and the corresponding maleinated SEBS-*g*-MA (Kraton FG1901X, grafted with 2 wt % maleic anhydride). Aminopropyl-functional glass beads (Potters-Ballotini 5000 CP-03, average diameter of 5 $\mu$m), containing 0.02 wt % coating of aminopropyltrimethoxysilane were used as filler component. 0.2 wt % Irganox 1010/Irgafos 168 (4/1 wt %) were added as stabilizer during melt processing.

### Preparation of Hybrid Composites

All composites were prepared under identical mixing and molding conditions. SEBS and SEBS-*g*-MA volume fractions were varied between 0 and 20 vol%. The filler content was maintained at 10 vol%. Melt blending was performed in a Haake Rheomix 90 twin-screw kneader equipped with a 60-mL mixing chamber that was preheated at 240°C. Typically, polypropene (PP) was molten together with the stabilizers for 1.5 min. Then the filler was added, followed 1 min later by SEBS and SEBS-*g*-MA, respectively. After 4 min of total mixing time, the sample was quickly recovered and quenched between metal plates. Sheets of 2 mm thickness for mechanical testings and of 1 mm thickness for rheological testings were prepared by compression molding in an evacuated press (Schwabenthan Polystat 100), annealing at 250°C for 10 min and quenching to room temperature between water-cooled metal plates. Rectangular bars of a dimension of 60 × 10 × 2 mm and 10 × 6 × 2 mm were cut out of these plates for evaluation of mechanical and dynamic mechanical properties. Circular specimen with 25 mm diameter were cut for rheological investigations.

### Mechanical and Dynamic Mechanical Testings

Tensile properties were measured on an Instron (Model 4202) tensile machine according to DIN 53455 standard procedure using a test specimen

of 2 mm thickness and a crosshead speed of 10 mm/min. The average standard deviations of Young's modulus and yield stress were approximately 5%. At least 5 samples were tested for each composite composition, and the average value is reported. Tests were performed at ambient temperature (23 ± 2°C). Dynamic mechanical testings were carried out with the aid of a Rheometrics Solid Analyser RSA II and dual-cantilever geometry (frequency, 1 Hz; heating rate, 2 K $min^{-1}$).

### Rheological Testings

The rheological behavior was studied using dynamic oscillatory tests in a Bohlin CVO rheometer with parallel plate fixtures of 25 mm diameter. The angular frequency $\omega$ was varied from 30 to $10^{-3}$ rad $s^{-1}$, and the temperature ranged from melting temperature plus 5°C (170°C) to 220°C, starting measurements with 220°C. All samples were studied under a nitrogen atmosphere in order to prevent thermooxidative degradation. The isotherms were shifted to obtain master curves at a reference temperature $T_0$ = 200°C using the program LSSHIFT.[11]

### Environmental Scanning Electron Microscopy

The morphology of the hybrid composites was determined by means of environmental scanning electron microscopy (ESEM). The fracture surfaces of impact tests were investigated using an electron microscope (Model 2020) of the Electro-Scan Corporation. The acceleration voltage was 20 kV.

## RESULTS AND DISCUSSION

### Morphology

Figure 2 shows ESEM images of fracture surfaces of i-PP hybrid composites with 10 vol% amino-functionalized glass beads and 5 vol% thermoplastic elastomer (TPE), eg., SEBS and SEBS-*g*-MA. Most of the fracture surface of hybrid composites containing 10 vol% glass beads and 5 vol% SEBS show the distinct structural features of nonadhering glass beads [Fig. 2(a)]. Due to weak interfacial adhesion, glass beads are pulled out of the matrix, leaving craters. ESEM images of hybrid composites containing 10 vol% glass beads and 5 vol% SEBS-*g*-MA clearly indicate that cracks travel predominately through the i-PP matrix [Fig. 2(b)]. The surface of the filler is very diffuse, thus reflecting formation of a SEBS-*g*-MA shell. This indicates, in accordance with results of crystallization behavior,[5] a three-phase morphology of SEBS-toughened, filled i-PP with separately dispersed glass beads and SEBS particles, whereas SEBS-*g*-MA-toughened, filled i-PP exhibits a two-phase morphology comprising core–shell particles.

### Mechanical Properties

Yield stress and Young's modulus of i-PP hybrid composites, measured as the first maximum and as the slope of the stress–strain curve, were determined as a function of TPE type and volume fraction. The dependence of relative yield stress, the quotient of composite yield stress, and the matrix yield stress on TPE volume fraction is depicted in Figure 3.

The yield stress of hybrid composites containing SEBS decreases with increasing TPE volume fraction. At small volume fraction of SEBS-*g*-MA of 5 vol%, a distinct yield stress increase was observed before encountering decays at higher SEBS-*g*-MA volume fractions. In comparison to SEBS, SEBS-*g*-MA gives much higher yield stresses and improved interfacial interactions due to in-situ filler encapsulation and improved interfacial adhesion. Previous research[5] has shown that approximately 2.5 vol% SEBS-*g*-MA is immobilized on the glass bead surface. In order to demonstrate the influence of separately dispersed SEBS-*g*-MA on yield stress, the values of the i-PP hybrid composites containing SEBS-*g*-MA were shifted to corresponding, reduced volume fractions. The dotted line in Figure 3 illustrates this shift procedure and indicates that separately dispersed SEBS and SEBS-*g*-MA have the same influence on tensile yield stress of i-PP hybrid composites. Thus, the improved yield stress of i-PP hybrid composites with SEBS-*g*-MA is caused by the elastomeric interlayer, improving interfacial adhesion.

In Figure 4, relative Young's modulus is plotted against TPE volume fraction. As expected, the hybrid composite moduli decrease with increasing TPE volume fraction. The stiffness of hybrid composites containing SEBS is always higher than that of corresponding hybrid composites containing SEBS-*g*-MA, especially at high TPE volume fractions. In the case of core–shell formation, as observed for SEBS-*g*-MA and glass beads in

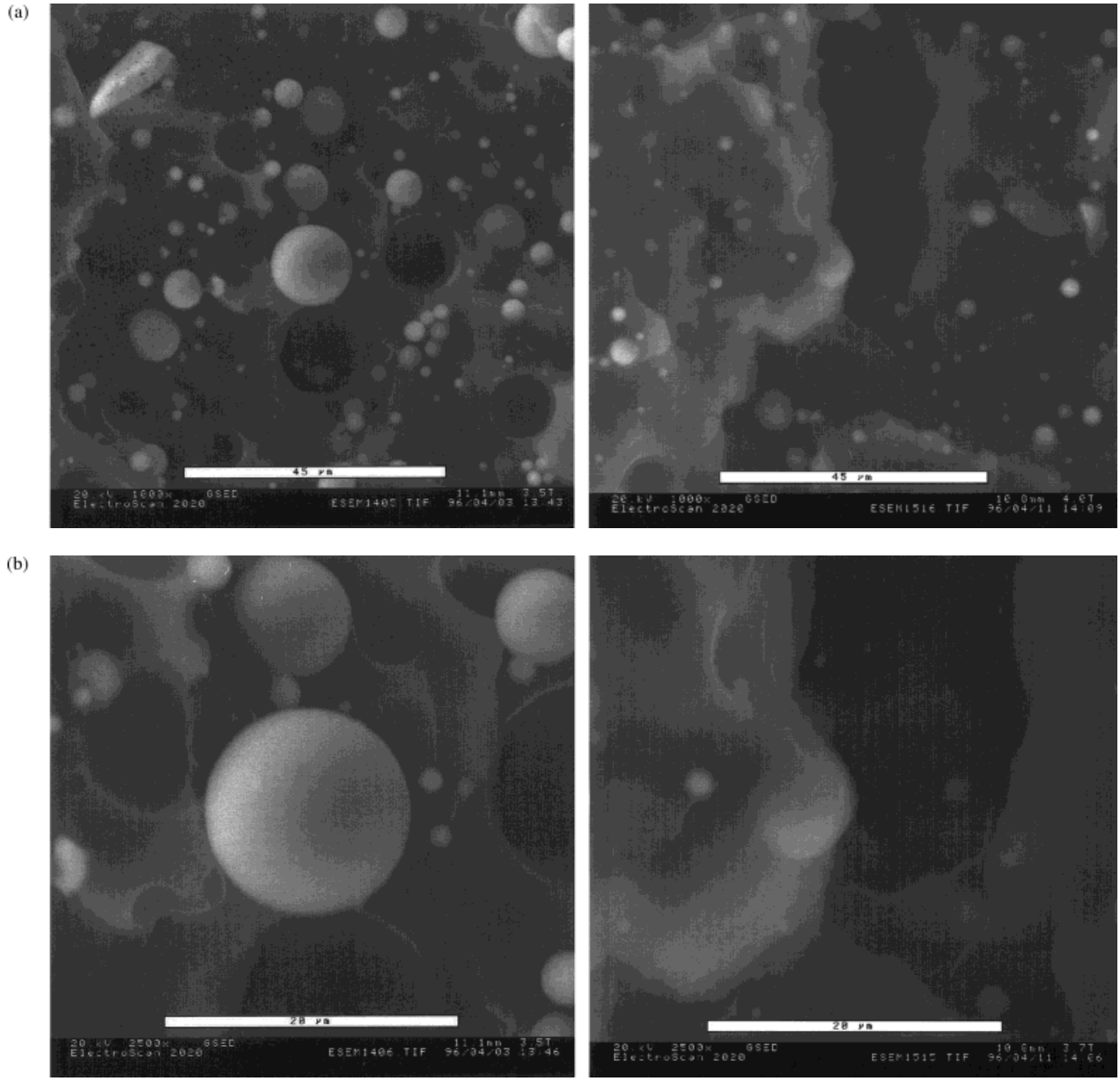


**Figure 2** Environmental scanning electron micrographs of fractured surfaces of i-PP hybrid composites containing (a) 10 vol% glass beads and 5 vol% SEBS and (b) 10 vol% glass beads and 5 vol% SEBS-*g*-MA.

i-PP, the effective TPE volume fraction increases while the stiffening effect of the filler is reduced with increasing thickness of the TPE shell. In correspondence to Figure 3, the dotted line illustrates the influence of separately dispersed SEBS-*g*-MA on Young's modulus. Because of the reduced stiffening effect of the glass beads, Young's moduli of hybrid composites with SEBS-*g*-MA are shifted to lower values, but the order of magnitude corresponds to that of hybrid composites with SEBS.

## Dynamic Mechanical Properties

Figure 5 shows the dynamic mechanical storage and loss moduli, $E'$ and $E''$, of i-PP hybrid composites containing 10 vol% glass beads and 10 vol% TPE as a function of temperature and TPE type.

As expected, the storage modulus decreases with increasing temperature. Incorporation of 10 vol% SEBS reduces the storage and loss modulus over the whole range of temperature. The sepa-

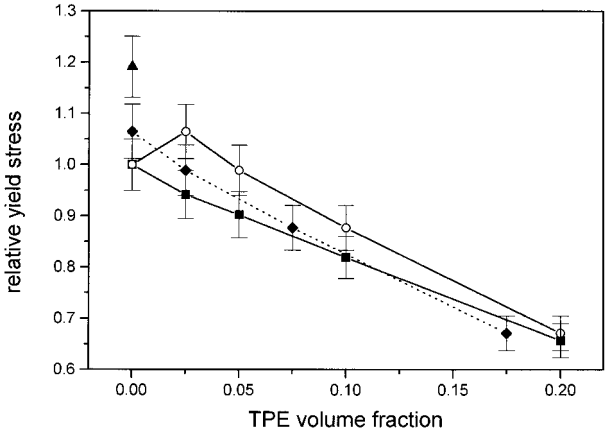


**Figure 3** Relative yield stress as a function of the TPE volume fraction of i-PP hybrid composites: (▲) i-PP; (■) i-PP with 10 vol% glass beads and SEBS; (○) i-PP with 10 vol% glass beads and SEBS-*g*-MA; and (♦) i-PP with 10 vol% glass beads and SEBS-*g*-MA volume fraction after shift procedure, considering the fixing of 2.5 vol% SEBS-*g*-MA on the glass bead surface (details in text).

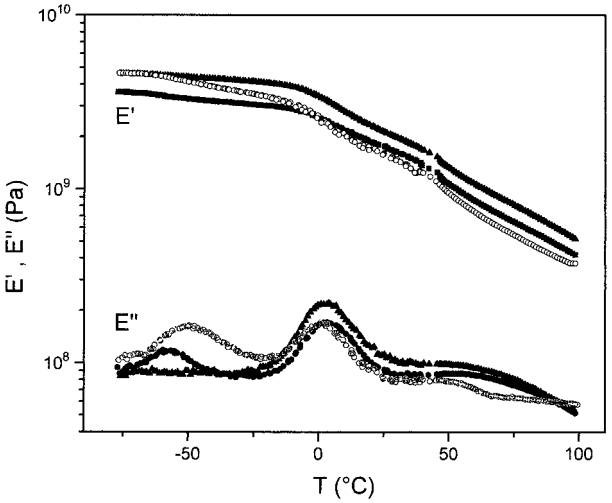


**Figure 5** Temperature dependence of dynamic mechanical storage and loss modulus $E'$ and $E''$ of i-PP hybrid composites: (▲) i-PP; (■) i-PP with 10 vol% glass beads and 10 vol% SEBS; and (○) i-PP with 10 vol% glass beads and 10 vol% SEBS-*g*-MA.

rate dispersed glass beads and SEBS particles influence the moduli of i-PP independent of each other. Below the glass transition temperature of SEBS-*g*-MA ($T_g$ equals −51°C) detected as the first maximum of loss modulus, the storage modulus of filled i-PP is unaffected by addition of 10 vol% SEBS-*g*-MA. Above this temperature, 10 vol% SEBS-*g*-MA lowers the storage modulus in comparison to the TPE-free composite. Near the glass transition of i-PP $T_g$ equals 4°C, storage and loss moduli of hybrid composites with SEBS-*g*-MA sink under the values of corresponding hybrid composites containing SEBS. Below the $T_g$ of TPE, the stiffening effect of the glass beads is uneffected by the SEBS-*g*-MA shell. With increasing temperature, the SEBS-*g*-MA shell gets softer and, as a consequence, the moduli of the hybrid composites decrease under the moduli of corresponding hybrid composites containing SEBS. At room temperature, hybrid composites with SEBS-*g*-MA have the lowest storage moduli, as also observed for Young's modulus. Beside mechanical and dynamic mechanical properties of i-PP hybrid composites, the flow behavior of the corresponding melts was investigated.

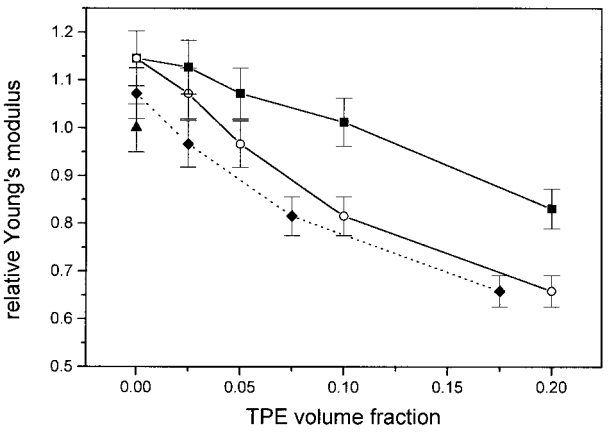


**Figure 4** Relative Young's modulus as a function of the TPE volume fraction of i-PP hybrid composites: (▲) i-PP; (■) i-PP with 10 vol% glass beads and SEBS; (○) i-PP with 10 vol% glass beads and SEBS-*g*-MA; and (♦) i-PP with 10 vol% glass beads and SEBS-*g*-MA volume fraction after the shift procedure, considering the fixing of 2.5 vol% SEBS-*g*-MA on the glass bead surface (details in text).

## Thermorheological Behavior

It is well known that the rheology of polymer melts strongly depends on temperature. In the case of thermorheological simplicity, isotherms of $G'(\omega, T)$ and $G''(\omega, T)$ can be superimposed by horizontal shifts along the frequency axis $\omega$. Usually, 2 empirical equations, the Arrhenius and the Williams-Landel-Ferry (WLF) equations, are used to describe temperature dependence of the shift factors. Arrhenius correlates the horizontal shift factor $a_T$ with the Arrhenius activation energy $E_{Arr}$ of the flow process, as follows:

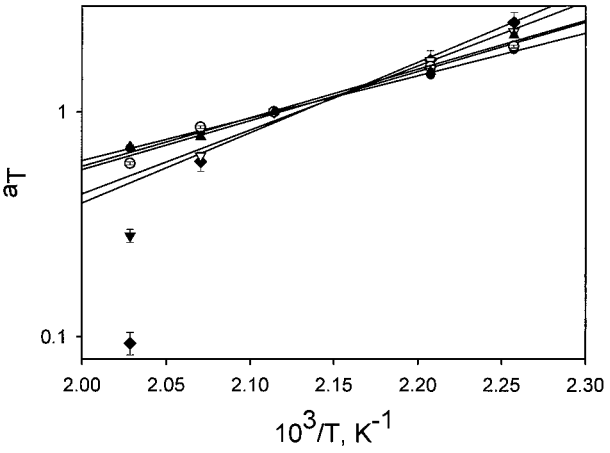


**Figure 6** Temperature dependence of the shift factors $a_T$ of i-PP filled with 10 vol% glass beads and SEBS and SEBS-*g*-MA, respectively, at a reference temperature of $T_0$ = 200°C: (■) no SEBS or SEBS-*g*-MA; (○) 10 vol% SEBS; (▲) 20 vol% SEBS; (▽) 10 vol% SEBS-*g*-MA; and (♦) 20 vol% SEBS-*g*-MA. The straight lines are calculated by the Arrhenius equation.

$$\log a_T = \frac{E_{\mathrm{Arr}}}{2.303\mathrm{R}}\left(\frac{1}{T} - \frac{1}{T_0}\right) \qquad (1)$$

where R is the universal gas constant (R = 8.314 J mol$^{-1}$). The WLF equation relates the shift factor $a_T$ with two coefficients, $c_1$ and $c_2$, as follows:

$$\log a_T = \frac{-c_1(T - T_0)}{c_2 + (T - T_0)} \qquad (2)$$

According to Lomellini[12] and Kulkarni and Mashelkar,[13] the WLF equation is valid up to $T_g$ + 300 K. Figure 6 shows the shift factors $a_T$ of i-PP hybrid composites in dependence on temperature, where the Arrhenius presentation log $a_T$ versus $1/T$ was used.

Shift factors $a_T$ are, as expected, increase with a decrease in temperature. At low temperatures, $a_T$ also increases with an increase in the TPE volume fraction. In comparison to SEBS, higher values of $a_T$ are obtained by incorporating SEBS-*g*-MA. At higher temperatures, the shift factor $a_T$ shows an inverse behavior: $a_T$ decreases with an increase in the TPE volume fraction. i-PP hybrid composites containing SEBS-*g*-MA have, at 220°C, extremely low shift factors $a_T$, which cannot be explained at the moment. Most likely, this effect results from the experimental procedure and is not considered further. Temperature variation leads only to a horizontal shift; thus the vertical shift factor $b_T$, not presented in Figure 6, is constant and equal to 1. As clearly seen, shift factors $a_T$ and, thus, flow behavior of filled i-PP with different amounts of SEBS and SEBS-*g*-MA, can be described well by the Arrhenius equation. Because of the good validity of the Arrhenius equation with a single fit parameter and the low shift factors of i-PP, the WLF equation with 2 fit parameters is not used in this study.

In Figure 7, the Arrhenius activation energy $E_{\mathrm{Arr}}$, determined by eq. (1), is plotted against the TPE volume fraction. Incorporation of 10 vol% glass beads effects the Arrhenius energy only marginally. The addition of SEBS to i-PP and glass-bead-filled i-PP slightly increases the Arrhenius energy. A distinct increase in activation energy is observed with SEBS-*g*-MA. Because of the enhanced interfacial interactions in glass-bead-filled i-PP containing SEBS-*g*-MA, the glass beads are efficient in hindering the flow processes of i-PP.

## Rheological Properties

Figures 8 and 9 show master curves of storage and loss moduli, $G'$ and $G''$, of i-PP blends with SEBS in dependence of angular frequency $a_T\omega$.

The curves result from the temperature shift procedure. It is obvious that the characteristic relaxation regions are obtained for all temperatures and composition with the flow region for lowest and the plateau region for the highest frequencies. Both regions are separated by a broad transi-

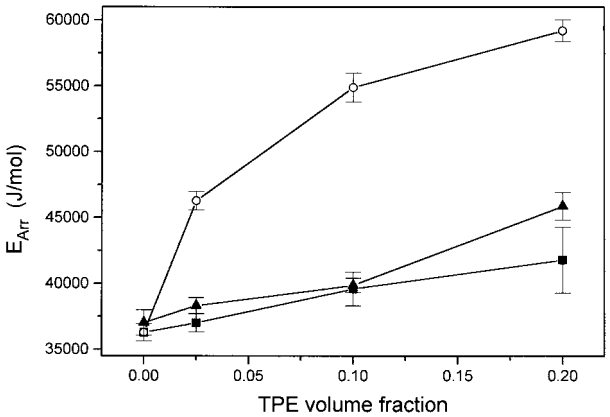


**Figure 7** Dependence of the Arrhenius activation energy $E_{\mathrm{Arr}}$ on the TPE volume fraction of i-PP blends and hybrid composites: (▲) i-PP with SEBS; (■) i-PP with 10 vol% glass beads and SEBS; and (○) i-PP with 10 vol% glass beads and SEBS-*g*-MA.

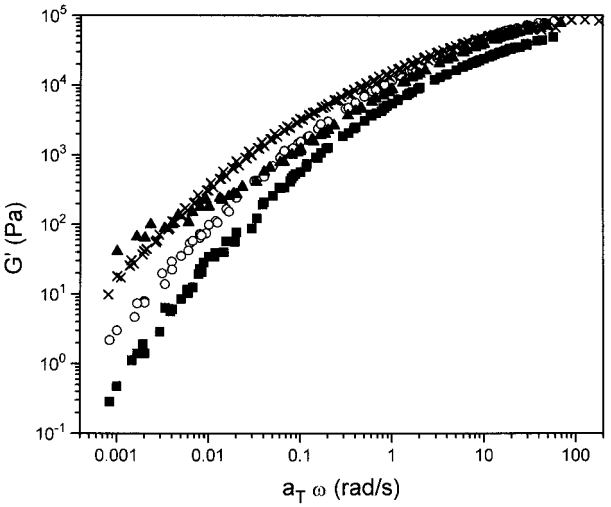


**Figure 8** Master curves of storage modulus $G'$ of i-PP blends with TPE versus reduced angular frequency $a_T\omega$ at the reference temperature of $T_0$ = 200°C: (■) i-PP; (○) i-PP with 10 vol% SEBS; (▲) i-PP with 20 vol% SEBS; and (X) SEBS.

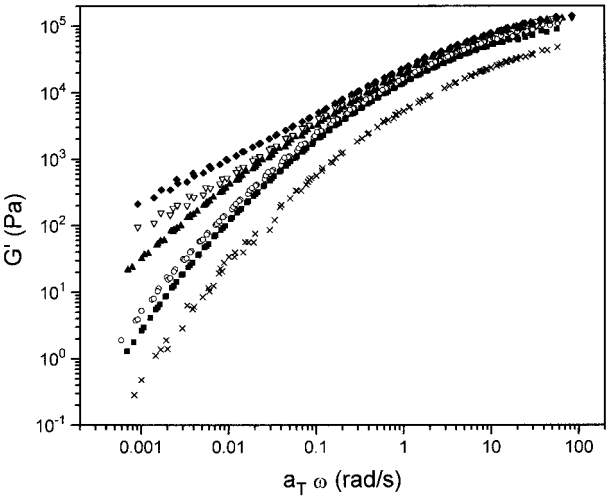


**Figure 10** Master curves of storage modulus $G'$ of i-PP filled with 10 vol% glass beads and SEBS–SEBS-*g*-MA versus reduced angular frequency $a_T\omega$ at the reference temperature of $T_0$ = 200°C: (■) no SEBS–SEBS-*g*-MA; (○) 10 vol% SEBS; (▲) 20 vol% SEBS; (▽) 10 vol% SEBS-*g*-MA; and (♦) 20 vol% SEBS-*g*-MA.

tion, which is characteristic for polymer matrices with significant polydispersity. With increasing SEBS volume fraction, the moduli are increasing over the whole range of frequencies. Besides, melt viscosity, characterized as zero shear viscosity $\eta_0$ increases with an increase in SEBS the volume fraction. Corresponding i-PP blends with SEBS-*g*-MA show the same behavior. Master curves of storage and loss modulus, $G'$ and $G''$, of i-PP hybrid composites are plotted in Figure 10 and 11 against angular frequency $a_T\omega$. Incorporation of 10 vol% glass beads shifts storage and loss modulus of i-PP to higher values. Additional SEBS increases the moduli, especially at low frequencies. A stronger enhancement is observed by incorpo-

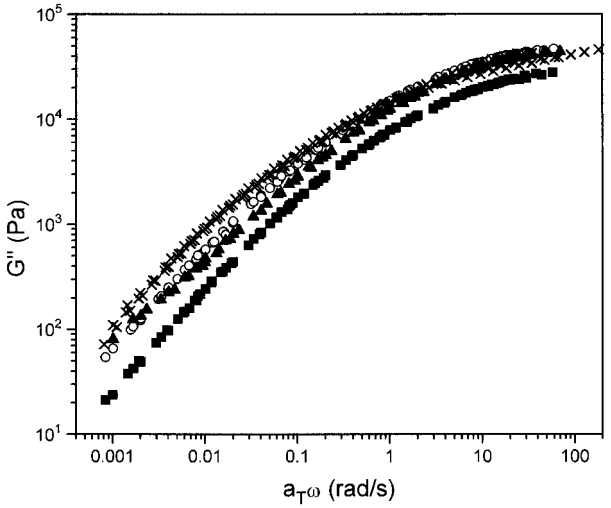


**Figure 9** Master curves of loss modulus $G''$ of i-PP blends with TPE versus reduced angular frequency $a_T\omega$ at the reference temperature of $T_0$ = 200°C: (■) i-PP; (○) i-PP with 10 vol% SEBS; (▲) i-PP with 20 vol% SEBS; and (X) SEBS.

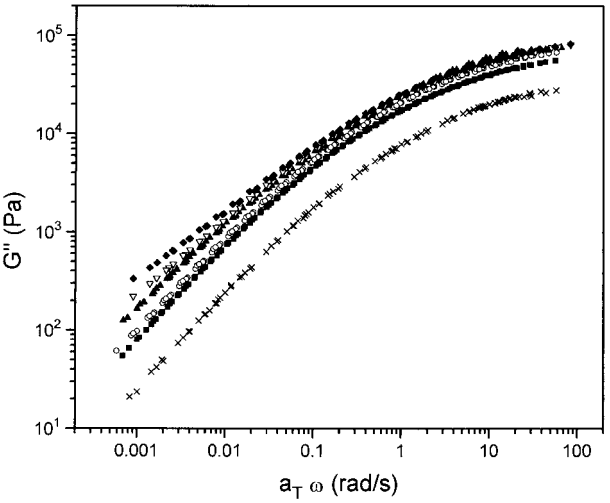


**Figure 11** Master curves of loss modulus $G''$ of i-PP filled with 10 vol% glass beads and SEBS–SEBS-*g*-MA versus reduced angular frequency $a_T\omega$ at the reference temperature of $T_0$ = 200°C: (■) no SEBS–SEBS-*g*-MA; (○) 10 vol% SEBS; (▲) 20 vol% SEBS; (▽) 10 vol% SEBS-*g*-MA; and (♦) 20 vol% SEBS-*g*-MA.

rating SEBS-*g*-MA instead of SEBS. The resulting core–shell morphologies increase the moduli as well as the viscosity more pronouncedly than separately dispersed glass beads and SEBS particles. The curves show that the rheological behavior strongly depends on the morphology of the hybrid composites. In accordance with the yield stress of hybrid composites in a solid state, enhanced interfacial interactions due to the SEBS-*g*-MA interlayer increase the viscosity of the hybrid composites, characterized by loss modulus $G''$. In contrast to results from mechanical testings on solid specimen with a reduced stiffening effect of the filler by the SEBS-*g*-MA interlayer, in melt, the interlayer enhances the storage modulus of i-PP hybrid composites significantly. This is in accordance with new results by Vignaux-Nassiet et al.,[14] who demonstrated that adsorbed polymers at the interface change the rheological response in the same manner as described here.

## CONCLUSION

The morphology of i-PP hybrid composites with glass beads and SEBS and SEBS-*g*-MA, respectively, strongly influences mechanical and rheological properties. A three-phase morphology was found for i-PP hybrid composites with glass beads and SEBS, whereas SEBS-*g*-MA forms core–shell morphologies with elastomeric interlayers between glass beads and the i-PP matrix.

Mechanical and dynamic mechanical experiments reflect a decrease in elasticity of i-PP hybrid composites due to the addition of the less elastic SEBS and SEBS-*g*-MA to the composite. Due to the SEBS-*g*-MA core around the glass beads, the stiffness of the i-PP hybrid composites is reduced and interfacial adhesion and, consequently, tensile yield stress, are improved when compared with i-PP hybrid composites with SEBS. In rheological investigations, the increased elasticity reflects the stronger interactions between the i-PP matrix and the glass beads promoted by the SEBS-*g*-MA interlayer.

It can be concluded that the melt elasticity and tensile yield stress of i-PP hybrid composites are strongly influenced by interfacial interactions between the components, whereas mechanical elasticity is mostly influenced by stiffness of the components.

The authors thank Shell Research in Ottignies-Louvain-la-Neuve, Belgium, for supporting this study.

## REFERENCES

1. Y. S. Lipatov, *Polymer Reinforcement,* ChemTec Publishing, Ontario, 1995.
2. E. Martuscelli, in *Polypropylene: Structure, Blends, and Composites,* Vol. 2, J. Karger-Kocsis, Ed., Chapman & Hall, London, 1995, p. 95.
3. J. E. Stamhuis, *Polym. Comp.,* **5,** 202 (1984).
4. J. E. Stamhuis, *Polym. Comp.,* **9,** 72 (1988).
5. F. Stricker and R. Mülhaupt, *J. Appl. Polym. Sci.,* **62,** 1799 (1996).
6. J. Kolarik and J. Jancar, *Polymer,* **33,** 4961 (1992).
7. A. K. Gupta and S. N. Purwar, *J. Appl. Polym. Sci.,* **29,** 1079 (1984).
8. J. E. Stamhuis and J. P. A. Loppé, *Rheol. Acta,* **21,** 103 (1982).
9. P. R. Hornsby and A. Mthupha, *J. Mater. Sci.,* **29,** 5293 (1994).
10. C. Friedrich, W. Scheuchenpflug, S. Neuhäusler, and J. Rösch, *J. Appl. Polym. Sci.,* **57,** 499 (1995).
11. J. Honerkamp and J. Weese, *Rheol. Acta,* **32,** 57, (1993).
12. P. Lomellini, *Polymer,* **33,** 4983 (1992).
13. M. G. Kulkarni and R. A. Mashelkar, *Polymer,* **22,** 867 (1981).
14. V. Vignaux-Nassiet, A. Allal, and J. P. Montford, *Eur. Polym. J.,* to appear.